Letters in Applied NanoBioScience
Open-Access Journal (ISSN: 2284-6808)

Article
Volume 15, Issue 1, 2026, 45
https://doi.org/10.33263/LIANBS151.045

Synthesis, Characterization, Electrochemical and Biological Evaluation of Binuclear Cu(II) Complexes with Novel Unsymmetrical Macrocyclic Ligands

Vedavalli Sairaj [1], Suvitha Athisaya Rajah [2,*], Iqbal Pakrudheen [3], Amani Alhejely [4], Rabab A. hegazy [5], Herri Trilaksana [6,*]

1 Department of Chemistry, Sea College of Science, Arts and Commerce, affiliated with Bangalore North University, Bengaluru, India
2 Department of Physics, CMR Institute of Technology, Bengaluru, 560037, India
3 Visvesvaraya Technological University (VTU), Belagavi, Karnataka, India
4 Centre of Excellence- Materials & Sensors, Department of Chemistry, CMR Institute of Technology, Bengaluru 560037, India
5 Biology Department, University College of Al-Darb, Jazan University, P.O. Box 114, Jazan 45142, Kingdom of Saudi Arabia
6 Department of Physics, Faculty of Science and Technology, Airlangga University, Surabaya 60115, Indonesia
* Correspondence: suvitha@cmrit.ac.in (S.A.R.); herri-t@fst.unair.ac.id (H.T.);

Received: 10.12.2024; Accepted: 24.02.2026; Published: 30.03.2026

Abstract: [Cu_2L_{1-5}] are five novel binuclear Cu(II) complexes. $2ClO_4$ with different new unsymmetrical binucleating macrocyclic ligands were synthesized by cyclocondensation between N, N'-bis(3- formyl-5-methylsalicylidene) alkane/benzene/naphthalene-diimines (PC1-5) and 3,4-diamino-pyridine in the presence of copper(II) acetate and copper(II) perchlorate (1:1:1:1 molar ratio). Elemental analysis, electronic and mass spectrum investigations, and FT-IR have been utilized to characterize these compounds. Cyclic voltammetry was used to examine the electrochemical properties of the complexes. At the cathodic potential range of 0 to -1.8 V, two quasireversible reduction waves are observed in all binuclear complexes. The complexes have two reduction potentials: one ranging from -0.50 to -0.75 V and the other from -0.85 to -1.25 V. Viscosity and spectral measurements have been made of the complexes' interactions with DNA. The Cu(II) complexes bind to DNA via an intercalative mechanism, as determined by absorption spectroscopy. The binding constants (Kb) for complexes 1–5 are 11.3 x 10^3, 12.0 x 10^3, 6.9 x 10^3, 11.7 x 10^3, and 7 x 10^3 M^{-1}, respectively. The Cu(II) complexes may alter the fluorescence of ethidium bromide and bind to DNA, as demonstrated by fluorescence spectroscopy. For complexes 1–5, the binding constants (K_{app}) are 3.1 x 10^5, 3.12 x 10^5, 3.14 x 10^5, 3.25 x 10^5, and 3.3 x 10^5 M^{-1}, respectively. More CD bands at 245 and 275 nm indicate that complex DNA binding is occurring effectively. UV-Vis absorption and fluorescence spectroscopy were employed to study the interaction of the complexes with BSA, showing a strong ability to quench BSA's fluorescence. The quenching mechanism was found to be predominantly static. Additionally, agarose gel electrophoresis experiments indicate that the compounds are highly effective in hydrolytic DNA cleavage. The MTT (3-(4,5-dimethylthiazol-2-yl)-2,5-diphenyl-tetrazolium bromide) assay was used to evaluate the impact of the complexes on cell viability. In human cervical MCF-7 cells, the dicopper(II) complexes 1-3 display cytotoxicity, with IC_{50} values of 10.7, 6.35, and 4.08 μM, respectively.

Keywords: Cu(II) complexes; unsymmetrical binucleating ligands; DNA/BSA interactions; cytotoxicity; redox properties; DNA cleavage.

1. Introduction

The study of interactions between transition metal complexes and DNA has become a significant area of research in bioinorganic chemistry, particularly following the discovery of cisplatin as an effective anticancer agent [1-8]. While cisplatin is highly effective in treating various cancers, its use is limited by significant dose-related side effects and the development of acquired or inherited resistance, which newer platinum-based drugs only partially address [9-12]. These challenges have led chemists to explore alternative strategies involving other transition metals with improved pharmacological profiles and mechanisms of action [13]. In recent years, the DNA-binding and cleavage properties of various transition metal complexes have received considerable attention. While many mononuclear complexes have been extensively studied, relatively few reports address binuclear systems [14-24]. Macrocyclic polyamine ligands containing two phenolic groups are of particular interest due to their high nuclease activity and ability to chelate metal ions in a spatially controlled fashion [25-27]. Binuclear copper(II) complexes supported by such macrocycles often exhibit enhanced DNA binding and redox behavior due to synergistic interactions between the two metal centers [28-30]. Recent studies on binuclear Cu(II) complexes have demonstrated potent DNA/BSA binding, ROS-mediated oxidative DNA cleavage, enzyme-mimicking behavior, and anticancer activity, including in colon and breast cancer models [31-33]. Furthermore, asymmetry in macrocyclic ligand frameworks can influence overall geometry, redox potential, and biological selectivity of the resulting complexes. This spatial asymmetry may enhance targeting of biological macromolecules by optimizing the arrangement of donor atoms and reactive centers. Recent reviews emphasize that steric and electronic asymmetry in copper complexes contribute to biological efficacy and ROS-generating pathways [34-38].

Therefore, the design of novel unsymmetrical binuclear macrocyclic Cu(II) complexes is a promising strategy to tune their structural and electronic properties and thereby enhance bioactivity. This work reports the synthesis and characterization of such complexes and investigates their DNA/BSA binding, redox properties, DNA cleavage activity, and cytotoxic effects.

2. Materials and Methods

2.1. Materials.

The synthesis of Robson-type macrocyclic dicopper(II) complexes was carried out, and copper(II) perchlorate hexahydrate, 3,4-diaminopyridine, and ethidium bromide (EB) were purchased from Aldrich. [39]. Acetonitrile and dimethylformamide (HPLC grade) were used as solvents for spectroscopic studies. CT-DNA and pBR322 DNA were purchased from Bio-Genics, Bangalore (India). Fluka supplied the tetra(n-butyl)ammonium perchlorate (TBAP), which was recrystallized from heated methanol. (Warning: TBAP may be explosive.); therefore, care must be taken when handling this compound.)

A CHI 600A power analyzer with a three-electrode configuration, a glassy carbon working electrode, a platinum wire counter electrode, and an Ag/AgCl reference electrode was used to conduct cyclic voltammetry. The scan rate ranged from 25 to 100 mV s^{-1}. Electrochemical measurements were conducted in DMF solutions containing 0.1 M TBAP as the supporting electrolyte, with complex concentrations ranging from 3 to 10 μM. The solution was cooled for 15 minutes prior to measurement.

Elemental analysis was carried out on a Carlo Erba Model 1106 Elemental Analyzer. FT-IR spectral data were collected using a Perkin-Elmer 2000 FTIR spectrometer, with samples prepared as potassium bromide (KBr) pellets. Absorption bands were recorded in the 200–750 nm range using a Perkin-Elmer Lambda 35 spectrophotometer. Fluorescence spectra were collected using a Perkin Elmer LS-45 detector, and electrospray ionization mass spectrometry (ESI-MS) measurements were conducted with a Thermo Finnigan LCQ-6000 Advantage Max mass spectrometer. Circular dichroism (CD) spectra of DNA were recorded on a Jasco J-810 spectrophotometer. MTT (3-[4,5-dimethylthiazol-2-yl]-2,5-diphenyltetrazolium bromide) was obtained from Invitrogen, USA. Acridine orange was obtained from Sigma, USA.

2.2. Methods.

2.2.1. Preparation of the precursor compounds.

2,6-diformyl-4-methylphenol was extracted according to a previously reported procedure [40]. The ligands N, N’-bis(3-formyl-5-methylsalicylidene)ethane-1,2-diimine (PC-1), N, N’-bis(3-formyl-5-methylsalicylidene)propane-1,3-diimine (PC-2), N, N’-bis(3-formyl-5-methylsalicylidene)butane-1,4-diimine (PC-3), N, N’-bis(3-formyl-5-methylsalicylidene)benzene-1,2-diimine (PC-4), and N, N’-bis(3-formyl-5-methylsalicylidene)naphthalene-1,8-diimine (PC-5) were synthesized following the procedure described in the literature [41].

2.2.2. Synthesis of mono and binuclear complexes.

Binuclear copper(II) complexes were synthesized from the respective precursor ligands (PC-1 to PC-5) via a stepwise protocol. Initially, each ligand was reacted with copper(II) acetate in a 1:1 molar ratio in a chloroform–methanol mixture (30:70, v/v) under reflux to yield the corresponding mononuclear complex. This was followed by a template condensation reaction, in which the formyl groups underwent Schiff-base condensation with 3,4-diaminopyridine in the presence of stoichiometric amounts of copper(II) perchlorate hexahydrate (Scheme 1).

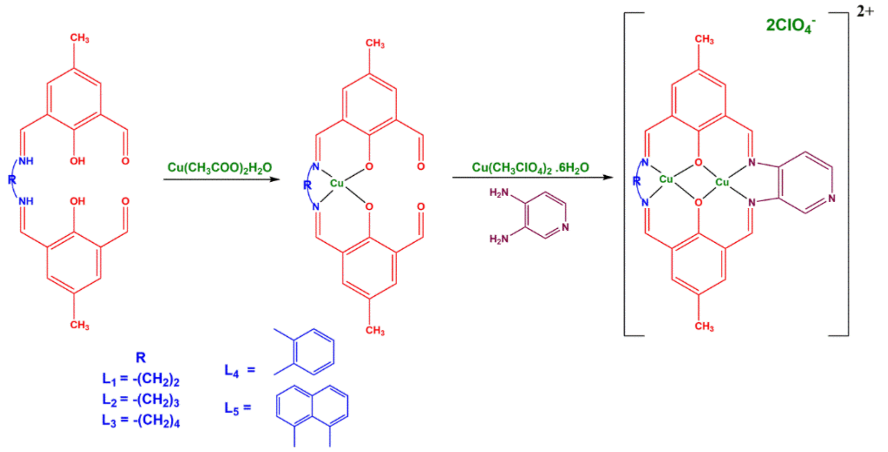

Scheme 1. Schematic representation for the synthesis of binuclear Cu (II) complexes $[Cu_2L_{1\text{-}5}]$ $(C1O_4)_2$.

2.2.2.1. $[Cu_2L_1](C1O_4)_2$.

A boiling solution of compound PC-1 (0.25 g, 0.07 mmol) in a chloroform–methanol mixture (30:70 v/v, 100 mL) was treated with copper(II) acetate monohydrate (0.14 g, 0.07

mmol), which had been previously dissolved in methanol (15 mL). The resulting mixture was refluxed for 30 minutes. Thereafter, a suspension of 3,4-diaminopyridine (0.076 g, 0.07 mmol) and copper(II) perchlorate hexahydrate (0.26 g, 0.07 mmol) in methanol (10 mL) was added to the precipitate formed. The reaction mixture was then refluxed for an additional 2 hours. During this period, the mononuclear complex was completely dissolved, affording a clear solution. After cooling to room temperature, the solution was filtered, and the filtrate was concentrated by evaporation. The resulting dark brown precipitate was collected by filtration, washed with cold methanol, and dried under vacuum.

Yield: (0.42 g, 80%); Colour: Dark brown; Anal.Calc. for: $C_{25}H_{21}N_5O_{10}Cl_2Cu_2$ (F.W. = 749.46 g/mol); Elemental analysis, calculated (%): C, 40.11; H, 2.81; Cu, 16.84; N, 9.36. Found: C, 40.05; H, 2.71; Cu, 16.75; N, 9.25.

2.2.2.2. $[Cu_2L_2]$ $(C1O_4)_2$.

The complex was prepared following the same procedure as described for complex 1, except that PC-2 (0.256 g, 0.07 mmol) was used in place of PC-1. Copper(II) acetate monohydrate (0.14 g, 0.07 mmol), 3,4-diaminopyridine (0.076 g, 0.07 mmol), and copper(II) perchlorate hexahydrate (0.26 g, 0.07 mmol) were employed in a chloroform–methanol mixture (30:70 v/v, 200 mL).

Yield: (0.43 g, 82%); Colour: Dark brown; Anal.Calc. for: $C_{26}H_{23}N_5O_{10}Cl_2Cu_2$ (F.W. = 763.49 g/mol); Elemental analysis, calculated (%): C, 40.94; H, 3.02; Cu, 16.53; N, 9.19. Found: C, 40.79; H, 2.95; Cu, 16.45; N, 9.15.

2.2.2.3. $[Cu_2L_3]$ $(C1O_4)_2$.

The complex was prepared using the same procedure as for complex 1, with compound PC-3 (0.266 g, 0.07 mmol) in place of PC-1. The ligand was dissolved in a chloroform–ethanol mixture (30:70 v/v, 150 mL).

Yield: (0.45 g, 85%); Colour: Dark brown; Anal.Calc. for: $C_{27}H_{25}N_5O_{10}Cl_2Cu_2$ (F.W. = 777.51 g/mol); Elemental analysis, calculated (%): C, 41.75; H, 3.22; Cu, 16.23; N, 9.02. Found: C, 41.65; H, 3.16; Cu, 16.18; N, 8.95.

2.2.2.4. $[Cu_2L_4]$ $(C1O_4)_2$.

The complex was prepared using the same procedure as for complex 1, with compound PC-4 (0.300 g, 0.07 mmol) in place of PC-1. The ligand was dissolved in a chloroform–ethanol mixture (30:70 v/v, 150 mL).

Yield: (0.47 g, 87%); Colour: Dark brown; Anal.Calc. for: $C_{29}H_{21}N_5O_{10}Cl_2Cu_2$ (F.W. = 797.50 g/mol); Elemental analysis, calculated (%): C, 34.45; H, 3.25; Cu, 15.85; N, 7.00. Found: C, 34.55; H, 3.30; Cu, 15.95; N, 7.05.

2.2.2.5. $[Cu_2L_5]$ $(C1O_4)_2$.

The complex was synthesized following the procedure described for complex 1, using compound PC-5 (0.33 g, 0.07 mmol) in place of PC-1. The ligand was dissolved in a chloroform–ethanol mixture (30:70 v/v, 150 mL).

Yield: (0.45 g, 80%); Colour: Dark brown; Anal.Calc. for: $C_{33}H_{23}N_5O_{10}Cl_2Cu_2$ (F.W. = 847.56 g/mol); Elemental analysis, calculated (%): C, 34.45; H, 3.25; Cu, 15.85; N, 7.00. Found: C, 34.55; H, 3.30; Cu, 15.95; N, 7.05.

2.3. $[Cu_2L_{1-5}]^{2+}$ – DNA binding interaction studies.

2.3.1. Absorption spectral studies.

Absorption spectral titration experiments of CT-DNA with the complexes were performed using a Perkin Elmer Lambda 35 spectrophotometer. A stock solution of CT-DNA was prepared in a buffer containing 5 mM Tris-HCl and 50 mM NaCl at pH 7.2, and stored at 4 °C. The concentration of CT-DNA was estimated by recording its UV absorbance at 260 nm, employing a molar absorptivity (ε) value of 6600 M^{-1} cm^{-1} at this wavelength. The ratio of absorbance at 260 nm to 280 nm (A_{260}/A_{280}) was approximately 1.8, demonstrating that there was not enough protein contamination in the DNA solution [42].

Absorption titration experiments were conducted with a fixed concentration of complexes while systematically increasing the DNA concentration. Typically, 20 μL aliquots of the CT-DNA stock solution were incrementally added to a 2.0 mL solution of the complexes (30 μM), and the absorption spectra were recorded over the 200–500 nm range. The binding constant (K_b) was calculated using equation (1) [43].

$$\frac{[DNA]}{(\varepsilon_a-\varepsilon_f)} = \frac{[DNA]}{(\varepsilon_b-\varepsilon_f)} + \frac{1}{K_b\,(\varepsilon_b-\varepsilon_f)} \qquad (1)$$

In this context, εa, εf, and εb represent the ratio of Aobsd to [complex], the molar extinction coefficient of the unbound (free) complex, and the molar extinction coefficient of the complex in its fully bound state, respectively.

2.3.2. Fluorescence spectral investigations.

Optical spectroscopy experiments were performed using a PerkinElmer LS-45 spectrophotometer equipped with a 1 cm path-length cuvette. The interaction study was performed by maintaining ethidium bromide (EB) at 2 μM and CT-DNA at 4 μM in a buffer solution of 50 mM Tris-HCl / 1 mM NaCl (pH 7.2), while varying the concentrations of the complexes from 0 to 60 μM. The binding of the complexes to immobilized EB–CT-DNA was quantified at room temperature, with excitation at 510 nm. The apparent binding constant (K_{app}) was calculated using equation (2) [44]:

$$K_{EtBr}\,[\text{EB}] = K_{app}[\text{complex}] \qquad (2)$$

Where K_{EtBr} is 1×10^7 M^{-1}, [EB] = 2 μM, and [complex] is the concentration of the complex that causes 50% reduction in the emission intensity of EB.

2.3.3. Viscosity measurements.

Viscosity measurements were conducted using a Brookfield DV-II+ Pro analyzer at 25°C. The concentration of CT-DNA was maintained at 100 μM in a buffer solution (5 mM Tris-HCl / 50 mM NaCl, pH 7.2). The results were expressed by plotting $(\eta/\eta_0)^{1/3}$ against the ratio of [complex] to [DNA], where η represents the specific viscosity of DNA in the presence of the complexes at concentrations of 4, 8, 12, 16, and 20 μM, while η_0 corresponds to the viscosity of DNA in the absence of any complex [45].

2.3.4. Circular dichroism.

One practical method to evaluate conformational changes in nucleic acids upon interaction with complexes is circular dichroism (CD) spectroscopy [46]. Circular dichroism (CD) spectra of CT-DNA were recorded with and without the complexes across the wavelength range of 220 to 320 nm, using a scanning speed of 300 nm per minute.Data were collected at 0.1 nm intervals at room temperature, using a 3 mL quartz cuvette.

2.4. DNA cleavage studies.

Assays for the dissociation of pBR322 DNA (0.5 μg/μL) in the presence of Cu(II) complexes (5.0–100 μM) were conducted using agarose gel electrophoresis in a Tris-HCl/NaCl buffer (5 mM Tris-HCl, 50 mM NaCl, pH 7.2). In a typical experiment, 5 μL of supercoiled pBR322 DNA (50 μg/μL) prepared in 100 mM Tris-HCl (pH 7.2) was treated with varying concentrations of the complex (0–50 μM), and the volume was adjusted with Tris-HCl buffer to a final volume of 17.5 μL. The samples were loaded onto a 1% agarose gel containing 1 μg/mL ethidium bromide (EB) after incubation at 37°C for varying periods of time. Each sample was run in duplicate during the 30-minute electrophoresis process at 50 V in Tris-acetate-EDTA (TAE) buffer. DNA band intensities were visualized under UV light and documented using gel imaging techniques.

2.5. MTT assay cell culture.

Penicillin/streptomycin (250 U/mL) and 10% fetal bovine serum were added to Roswell Park Memorial Institute (RPMI) medium to culture MCF-7 human breast cancer cells, obtained from the National Center for Cell Science (NCCS), Pune. Gentamicin (100 μg/mL) and amphotericin B (1 mg/mL) were purchased from Sigma Chemicals. Cell cultures were maintained at 37°C in a humidified atmosphere containing 95% air and 5% CO_2. The cells were allowed to grow for 24 hours prior to experimental use.

2.5.1. Cytotoxicity assay.

The effects of the complexes on MCF-7 cell growth were evaluated using the rapid thiazolyl blue tetrazolium bromide (MTT) colorimetric assay [47]. MCF-7 cells were seeded at a density of 5×10^3 cells per well in 96-well plates and incubated for 24 hours with 200 μL of RPMI medium supplemented with 10% fetal bovine serum (FBS). The culture medium was then removed, and RPMI containing varying concentrations of the test compounds (0.11–100 μg/mL) was added, followed by incubation for an additional 48 hours. After treatment, the cells were incubated with MTT solution (10 μL, 5 mg/mL) at 37°C for 4 hours, after which dimethyl sulfoxide (DMSO) was added and incubated at room temperature for 1 hour to dissolve the formazan crystals. Absorbance was measured at 595 nm using a multiwell spectrophotometer. All data represent the average of six independent experiments. Cell viability (%) was calculated as (Mean OD / Control OD) × 100, and cytotoxicity was expressed as the half-maximal inhibitory concentration (IC_{50}).

3. Results and Discussion

3.1. Spectral analysis.

The ESI mass spectra of the positive ions for Cu(II) complexes 1–5 exhibited major peaks at *m/z* = 649, 663, 677, 697, and 747, corresponding to the $[Cu_2L_{1-5}\cdot ClO_4]^+$ ion. Additional peaks at *m/z* = 275, 282, 289, 299, and 324 confirmed the presence of the doubly charged $[Cu_2L_{1-5}]^{2+}$ core. The analytical mass spectra and ESI data are consistent with the proposed structures of the dicopper(II) complexes.

The dinuclear complexes displayed infrared (IR) spectra distinct from those of the corresponding precursor ligands (PC1–5). The effective formation of the Schiff base was indicated by a characteristic peak at approximately 1620 cm^{-1}, corresponding to the imine ν(C=N) stretch, alongside the disappearance of the aldehyde ν(HC=O) peak at around 1670 cm^{-1}. The dinuclear Cu(II) complexes 1–5 showed two peaks near 1100 cm^{-1} attributed to the antisymmetric stretch of perchlorate ions, and a peak near 630 cm^{-1} corresponding to the antisymmetric band of perchlorates. Of the two peaks near 1100 cm^{-1}, one exhibited splitting due to coordination with perchlorate ions. A broad band around 3400 cm^{-1} indicated the presence of lattice or coordinated water.

Two new bands were observed at 582–592 cm^{-1} and 440–461 cm^{-1}, which are assigned to M–O and M–N stretching vibrations, respectively, confirming metal–ligand bonding in the complexes. The electronic absorption spectra of the complexes in acetonitrile (CH_3CN) revealed three primary transitions. A weak band between 530 and 560 nm was attributed to the d–d transition of the Cu(II) ion, suggesting a distorted square pyramidal coordination geometry around the metal center in complexes 1–5 [48]. The most intense band, observed in the near-UV region (350–365 nm), was assigned to an overlap of the π–π* transition of the azomethine group with a charge transfer transition from the phenolate bridge to the d-vacant orbital of the Cu(II) ion. Additionally, a strong band at 260–270 nm was attributed to internal charge transfer.

3.2. Cyclic voltammetry.

Using cyclic voltammetry, the redox behaviour of complexes 1–5 was investigated in DMF with tetrabutylammonium perchlorate as the supporting electrolyte. A representative cyclic voltammogram for complex 5 is shown in Figure 1, and the corresponding electrochemical data are compiled in Table 1. All the complexes displayed two quasi-reversible reduction waves in the cathodic region. For each complex, the first redox couple appeared in the range of −0.50 to −0.75 V (vs. Ag/AgCl), while the second was observed between −0.85 and −1.25 V. Controlled potential electrolysis performed at 100 mV more negative than the peak potentials confirmed that both redox processes involve single-electron transfers (n ≈ 0.94), corresponding to the Cu(II)Cu(II)/Cu(II)Cu(I) and Cu(II)Cu(I)/Cu(I)Cu(I) redox couples, respectively.

$$Cu^{II}\text{-}Cu^{II} \longleftrightarrow Cu^{I}\text{-}Cu^{II} \longleftrightarrow Cu^{I}\text{-}Cu^{I}$$

The observed electrochemical behavior is consistent with literature values for related binuclear Cu(II) macrocyclic complexes, which typically exhibit first reduction potentials in the −0.40 to −0.70 V range and second reductions between −0.90 and −1.20 V, depending on ligand environment and solvent polarity. For instance, binuclear Cu(II) Schiff base complexes reported by Fei et al. and Sankar et al. exhibit similar redox potentials, supporting the assignment of mixed-valent species in our system [28,29]. The macrocyclic framework clearly influences redox potentials, particularly through variations in ring size and donor-atom arrangement. As shown in Table 1, a slight shift in reduction potential correlates with macrocycle rigidity and electronic environment, suggesting that the ligand's geometry modulates the Cu(II)/Cu(I) redox couple. These findings reinforce the structural control of redox properties in dinuclear copper systems.

Table 1. Electrochemical data[a] of binuclear copper(II) complexes in DMF medium.

Complex	E^1 pc (V)	E^1 (V) pa	E^1 (V) 1/2	ΔE^1(mV)	E^2 (V) pc	E^2 (V) pa	E^2 (V) 1/2	ΔE^2(mV)
1	-0.80	-0.62	-0.71	-180	-1.18	-1.00	-1.09	-180
2	-0.62	-0.42	-0.52	-200	-0.92	-0.82	-0.87	-100
3	-0.76	-0.60	-0.68	-160	-0.96	-0.84	-0.90	-120
4	-0.72	-0.52	-0.62	-200	-1.10	-0.96	-1.03	-140
5	-0.80	-0.64	-0.72	-160	-1.32	-1.14	-1.23	-180

[a] Measured by CV at 100 mV/s. E versus Ag/AgCl conditions: GC working and Ag/AgCl reference electrodes; supporting electrolyte TBAP; concentration of complex $1x10^{-3}$ M, concentration of TBAP $1x10^{-1}$ M

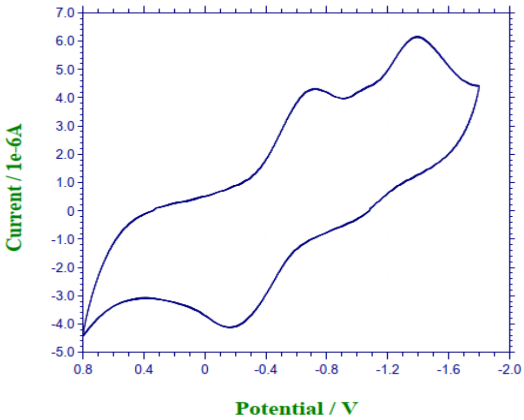

Figure 1. Cyclic voltammograms of the $[Cu_2L_5]$ $(ClO_4)_2$ in DMF solution with TBAP as supporting electrolyte.

3.3. Interaction of copper (II) complexes with DNA.

3.3.1. Cyclic voltammetric studies.

Cyclic voltammetry serves as a valuable complementary technique to UV–visible and fluorescence spectroscopy for investigating DNA-bound complexes [49,50].

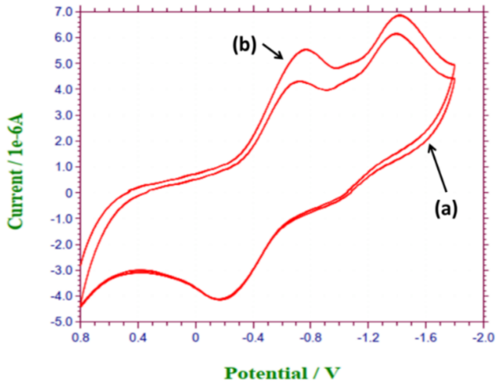

Figure 2. Cyclic voltammogram of the complex 5 in the absence (a) and presence (b) of CT-DNAin 50 mM Tris–HCl/50 mM NaCl buffer solution (pH = 7.2), scan rate: 0.1 V/s.

Figure 2 shows the cyclic voltammograms of the complexes recorded both in the absence and presence of CT-DNA. Upon addition of DNA at concentrations equivalent to $[Cu_2L]$, shifts in the half-wave potential ($E_{1/2}$) and peak-to-peak separation (ΔE) were observed. Additionally, an increase in DNA concentration led to a decrease in the cathodic-to-anodic peak current ratio (i_{pc}/i_{pa}). This reduction in peak current is likely due to an equilibrium between the free copper complex and DNA-bound species at the electrode surface, possibly driven by interactions between the planar aromatic groups of the DNA base pairs and the complex.

3.3.2. Absorption spectral studies.

Electron absorption spectroscopy is a highly effective technique for studying DNA binding interactions. Complexes can bind to DNA either by intercalation between base pairs or by interacting along the DNA backbone. Generally, simple binding results in minimal changes in absorption band intensity; consistent with this, no significant intensity changes were observed in such cases. However, intermediate binding interactions typically produce hypochromism (decreased absorption intensity) and a red shift (bathochromic shift) in the absorption bands.

The electronic spectra of the complexes exhibit two ligand-centered (LC) transitions: a π–π^* transition in the 350–365 nm region and an n–π^* transition in the 260–270 nm region. For UV-visible absorption titrations, copper(II) complexes were dissolved in DMF at a concentration of 5×10^{-5} M, while the concentration of CT-DNA was varied with the complex concentration held constant. Prior to measurement, the DNA–complex solutions were incubated at room temperature for 30 minutes, and spectra were recorded using a 1 cm path length cuvette.

As shown in Figure 3, the absorption peaks at 255 nm and 326 nm of the complex solution decreased upon the addition of DNA. The significant hypochromism, reaching up to 40% at the specified wavelengths, indicates an interaction between CT-DNA and the intercalating complexes. The intrinsic binding constant (K_b) was determined by analyzing the variation in absorbance at 255 nm with increasing CT-DNA concentration, thereby offering a quantitative assessment of the DNA-binding affinity of the complexes.In most cases, the electronic spectra of these complexes exhibited no radioactivity upon interaction with complementary DNA sequences. By analyzing absorbance changes at 255 nm for complexes 1–5 with increasing DNA concentration, intrinsic DNA binding constants (K_b) were determined to be 1.12×10^5, 1.20×10^5, 6.9×10^4, 7.0×10^4, and 1.17×10^5 M^{-1}, respectively. Comparison of the binding constants shows that complexes 4 and 5, which contain aromatic groups, exhibit enhanced DNA binding relative to complexes 1–3. This enhancement is likely linked to stronger interactions between transcription factors and the aromatic moieties.

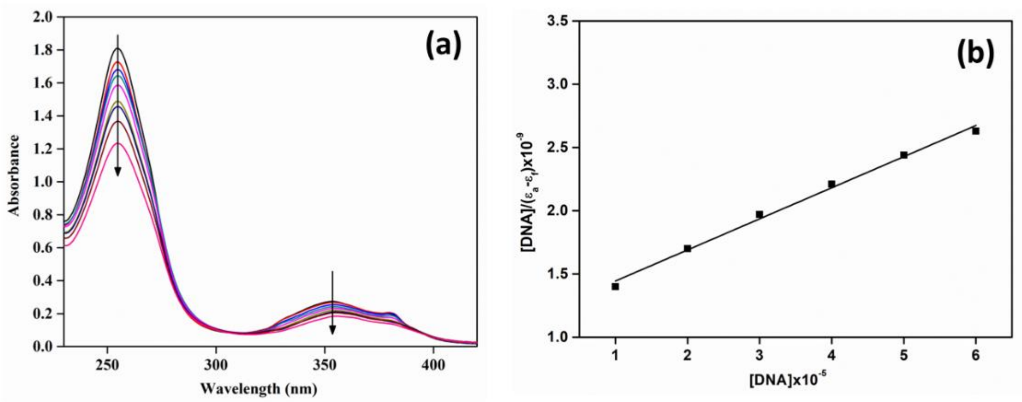

Figure 3. UV-visible spectra of the **(a)** Cu(II) complex in the presence of increasing amounts of CT-DNA in 50 mM Tris–50 mM NaCl aqueous buffer solution (pH = 7.2); **(b)** Plot of [DNA]/(ε_a - ε_f) versus [DNA] for absorption titration of CT-DNA with the complex.

3.3.3. Fluorescence spectroscopic studies.

Ethidium bromide (EB) intercalates between adjacent DNA base pairs, resulting in strong fluorescence in the presence of DNA. Previous studies have shown that the introduction of a second molecule can decrease this fluorescence intensity. The binding affinity of this second molecule to DNA can be evaluated by monitoring the fluorescence of EB bound to DNA. In dilution experiments, varying concentrations of the Cu(II) complexes were added to a 1.5 mL solution of EB-bound CT-DNA. All measurements were performed at ambient temperature using cuvettes with a 1 cm path length. The samples were excited at 510 nm, and the emission spectra were recorded over the range of 550–700 nm.

In our study, the fluorescence intensity showed a gradual decline with the incremental addition of Cu(II) complexes to the EB–DNA system. Figure 4 presents the emission spectra of EB bound to DNA, both in the absence and presence of these complexes. The significant reduction in fluorescence intensity upon complex addition indicates that the Cu(II) complexes interact with DNA by displacing EB, a characteristic behavior of intercalative DNA binding.

The apparent quenching constants (K_{app}) obtained for complexes 1–5, determined from the slopes of the Stern–Volmer plots (Figure 4), were 3.1×10^5, 3.12×10^5, 3.14×10^5, 3.25×10^5, and 3.3×10^5 M^{-1}, respectively. These values are comparable to those reported for DNA intercalative complexes [52], supporting the conclusion that the Cu(II) complexes bind to DNA via an intermediate intercalative mode.

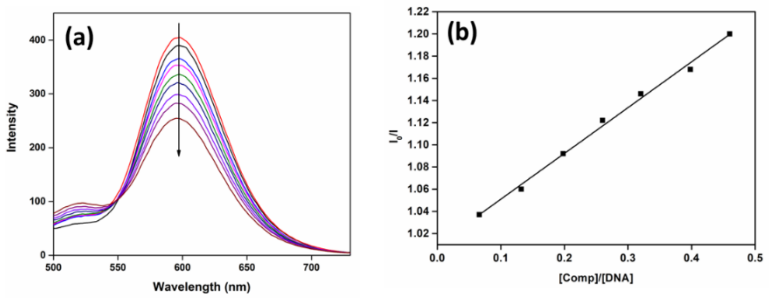

Figure 4. (a) Emission spectra of EB attached to DNA with and without complex 5; **(b)** Stern-Volmer quenching plot of EB bound to DNA by complex. I_0 represents the EB-DNA emission intensity when complex is not present, and I represents the EB-DNA emission intensity when complex is present.

3.3.4. Circular dichroism spectroscopy.

DNA binding of the Cu(II) complexes was also investigated using circular dichroism (CD) spectroscopy.

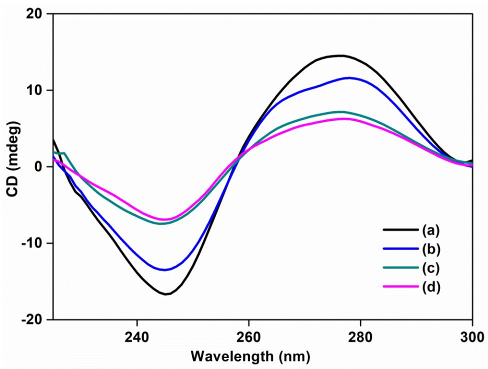

Figure 5. The circular dichromism spectra of CT-DNA in the absence **(a)** and presence of the complexes (b-complex 1, c-complex 2, d-complex 5). [CT-DNA] = 25 µM, [complex]/[DNA] = 0.5. All the spectra were recorded in Tris–HCl buffer, pH = 7.2.

CT-DNA typically adopts the B-DNA conformation, characterized by a negative CD band near 245 nm, attributable to the helical structure, and a positive CD band around 275 nm, corresponding to base stacking interactions [53]. Upon treatment of CT-DNA with the Cu(II) complex at a molar ratio of 0.5 ([complex]/[DNA]), significant alterations in the CD spectrum were observed. Specifically, the intensities of both the positive and negative bands changed (Figure 5), indicating disruption of the native CT-DNA structure. These results suggest that the complex binds to DNA and relaxes the helix [54].

3.3.5. Viscosity experiments.

A viscosity study was performed to elucidate further the interaction mechanism of the Cu(II) complexes with DNA. In the absence of structural information from X-ray crystallography or NMR, hydrodynamic methods, such as viscosity measurements, are particularly effective for investigating DNA-binding modes, as they are highly sensitive to changes in DNA length [55,56]. The addition of the complexes resulted in an increase in the viscosity of the CT-DNA solution.

Classical DNA intercalators, such as ethidium bromide (EB), cause a significant increase in the relative specific viscosity (η/η_0) of DNA solutions—where η and η_0 represent the viscosities of DNA in the presence and absence of the complexes, respectively—due to DNA elongation caused by base pair separation during intercalation [57,58]. In contrast, molecules that bind externally or within the grooves of DNA typically induce negligible or irregular changes in DNA viscosity [59]. The specific viscosity of the DNA solution increased significantly upon addition of the complexes, with relative viscosities rising as the concentration of the complexes increased. Figure 6 presents plots of the relative viscosity $(\eta/\eta_0)^{1/3}$ versus the [complex]/[DNA] ratio for the complexes. This increase in DNA viscosity is attributed to an intermediate binding mode of the complexes, supporting and extending the findings reported in previous studies [60,61].

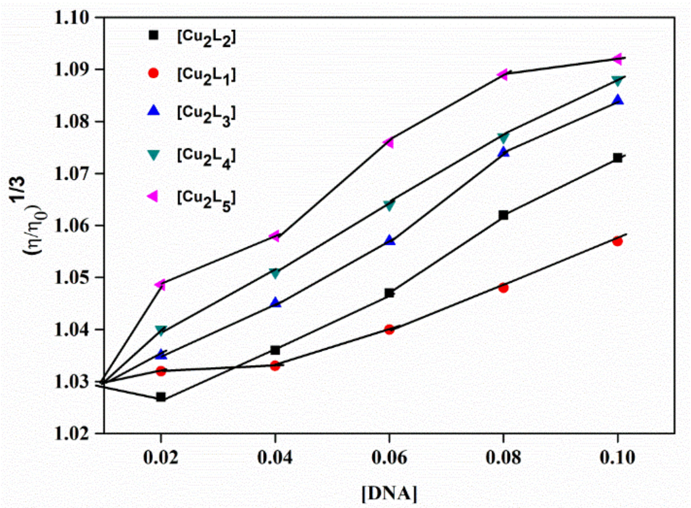

Figure 6. Effects of increasing amounts of the complex on the relative viscosities of CT-DNA at 23.0 (±0.1) ° C; [DNA] = 100 µM, r = [M]/[DNA].

The specific viscosity of the DNA sample increases significantly with the addition of the complexes, and the relative viscosity of the DNA increases as the concentration of the complexes increases. Figure 6 shows plots of relative viscosity $(\eta/\eta_0)^{1/3}$ against the [mixture]/[DNA] ratio for the complexes. This rise in DNA viscosity is attributed to the complex's intermediate binding mode, which supports the findings of the previous article [60,61].

3.4. Protein binding studies.

Bovine serum albumin (BSA) is widely employed in research due to its structural similarity to human serum albumin (HSA) [62,63]. As the most abundant plasma protein, BSA serves as a valuable model for studies on protein folding and synthesis in biotechnology. Given its biological relevance, BSA is frequently chosen as a binding protein and has become a key model for investigating drug–protein interactions. Understanding the binding interactions of compounds with albumins is essential for elucidating their pharmacokinetic and pharmacodynamic properties [64,65].

3.4.1. UV-visible absorption spectral analysis.

Evidence for static quenching can also be supported by UV-Vis spectral analysis of the fluorophore. In cases of dynamic quenching, the absorption spectrum of the fluorophore generally remains unchanged, as only the excited-state fluorescence is affected by the quencher. In contrast, static quenching involves interactions in the ground state, leading to the formation of a stable complex between the quencher and the fluorophore. This typically results in notable changes in the absorption spectrum.

Figure 7 illustrates the absorption spectra of free BSA and BSA in the presence of complex 5. BSA exhibits a characteristic absorption band at 280 nm. Upon addition of the Cu(II) complexes, a decrease in absorbance accompanied by a red shift in the spectra was observed. These findings suggest that the binding interaction between the Cu(II) complexes and BSA follows a static quenching mechanism.

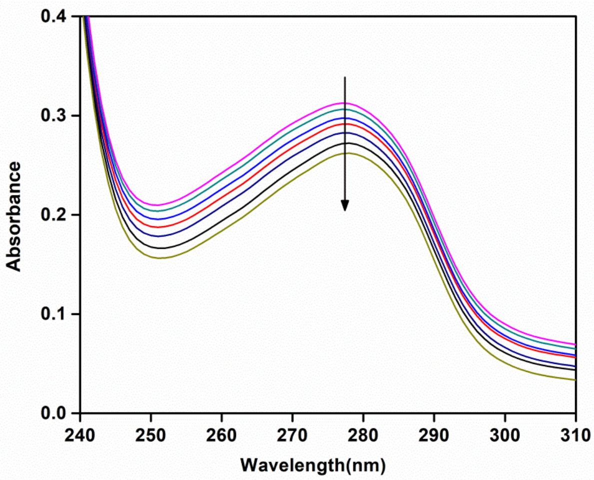

Figure 7. Absorption spectra of BSA in the presence of various concentrations of Cu(II) complex.

3.4.2. Fluorescence quenching of BSA.

Fluorescence spectroscopy is a valuable technique for investigating the interactions between metal complexes and bovine serum albumin (BSA), offering insights into local structural and dynamic changes within the protein. A decrease in fluorescence intensity often indicates complex formation between the metal complexes and BSA, which contains intrinsic fluorophores—primarily tryptophan residues such as Trp-134 and Trp-212. The emission intensity of BSA is influenced by the microenvironment of these residues, particularly their proximity to quenching groups such as carbon protons, imidazole protons, or tyrosine anions, which can affect molecular interactions.

In this study, the binding affinity of Cu(II) complexes 1–5 with BSA was examined under physiological conditions. Figure 8 demonstrates the effect of complex 5 on the fluorescence emission of BSA. Upon excitation at 280 nm, BSA exhibits a strong emission band centered around 360 nm. The addition of Cu(II) complexes led to quenching of BSA fluorescence, likely due to conformational changes in the protein's secondary or tertiary structure in phosphate buffer, altering the spatial orientation of tryptophan residues.

The binding constants (K_{BSA}) for complexes 1–5 were determined to be 3.2×10^5 M^{-1}, 4.6×10^5 M^{-1}, 6.3×10^5 M^{-1}, 6.8×10^5 M^{-1}, and 7.0×10^5 M^{-1}, respectively, indicating a strong and progressive affinity of the complexes for BSA.

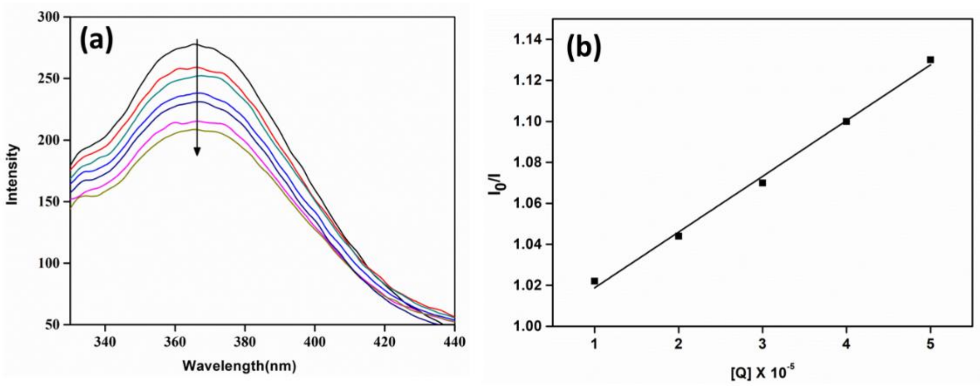

Figure 8. Fluorence spectra of **(a)** BSA in presence of various concentration of complex-5 Vs [Ikuta, #6187], [Ikuta, #6187]= 1×10^{-6} M^{-1}, [complex] = (0 - 10×10^{-6} M^{-1}); **(b)** Plot of [, #5196] versus (I_0/I) for emission titration of BSA protein with the complex.

3.5. Chemical nuclease activity.

To evaluate the DNA cleavage efficiency of complexes 1–5, supercoiled (SC) pBR322 DNA (100 ng/µL) was incubated with varying concentrations of the complexes in 5% DMF, prepared in Tris-HCl/NaCl buffer (50:5 mM, pH 7.2), for 30 minutes in the presence of hydrogen peroxide (H_2O_2) as an activator (Figure 9). Upon treatment with the Cu(II) complexes and H_2O_2, the supercoiled form of DNA (Form I) was progressively converted into nicked circular DNA (NC, Form II) and linear DNA (LC, Form III).

The extent of conversion from Form I to Forms II and III increased with increasing complex concentration, indicating concentration-dependent nuclease activity. Notably, the macrocyclic complexes containing additional aromatic moieties (complexes 4 and 5) exhibited enhanced DNA cleavage activity compared to the others, suggesting a possible correlation between aromaticity and nuclease efficiency.

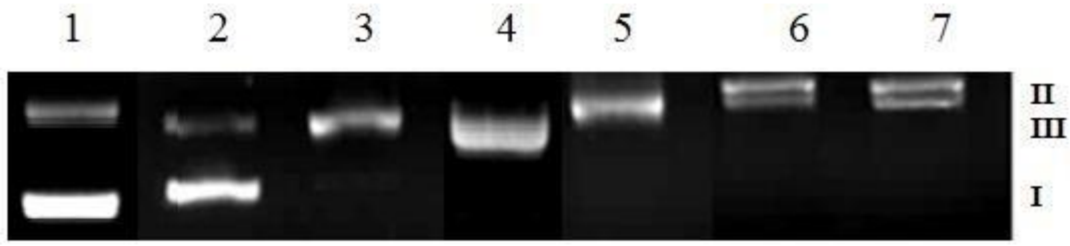

Figure 9. Cleavage of SC pBR322 DNA (0.1 lg) by Cu(II) complexes (15µg) in 50 mM Tris– HCl/NaCl buffer (pH 7.2). Lane 1: DNA control, lane 2: DNA +H_2O_2, lane 3: DNA + H_2O_2 + complex 1, lane 4: DNA + H_2O_2 +complex 2, lane 5: DNA + H_2O_2 +complex 3, lane 6: DNA + H_2O_2 +complex 4, lane 7: DNA + H_2O_2+complex 5.

3.5.1. Investigation of DNA cleavage in the presence of the activator and radical scavengers.

Gel electrophoresis experiments were conducted, and the graph (Figure 10) shows the separation of pBR322 supercoiled DNA (150 µg/mL) and Cu(II) complex 4 (0.06 mM) in the presence of various reagents: (50 mM) Tris-HCl buffer at pH 7.2 and 37°C. The dissociation activity of complex 4 was significantly reduced in the presence of DMSO, indicating that •OH was incorporated in the dissociation activity. The hydrogen peroxide adsorbent KI also significantly inhibited the dissociation activity of the compounds (lane 7), confirming that H_2O_2 was involved in the dissociation reaction. The singlet oxygen scavenger NaN_3 (lane 5) and the superoxide displacer SOD (lane 6) did not inhibit DNA cleavage, suggesting that $^1O_2$ and superoxide are not incorporated in the cleavage mechanism. Thus, these complexes appear to follow similar pathways in the cleavage process, in which hydroxyl radicals and hydrogen peroxide (H2O2) are important.

Based on the dependence on H_2O_2 and inhibition by DMSO and KI, the cleavage likely proceeds via an oxidative pathway involving hydroxyl radicals. The lack of inhibition by NaN_3 and SOD rules out significant contributions from singlet oxygen and superoxide species. However, a minor hydrolytic mechanism may also be present, as some cleavage is observed even in the absence of oxidants. These observations are consistent with previously reported Fenton-type oxidative mechanisms by Cu(II) macrocyclic or Schiff-base complexes, where radical scavengers such as DMSO suppress DNA cleavage, confirming the role of •OH as the active species. Similar oxidative cleavage mechanisms involving Cu(II) complexes and hydroxyl radicals have been reported in recent studies by Parsekar et al. and Paliwal et al. [66, 67], where ROS-mediated cleavage dominated in the presence of H_2O_2, while minimal hydrolytic contribution was observed in its absence

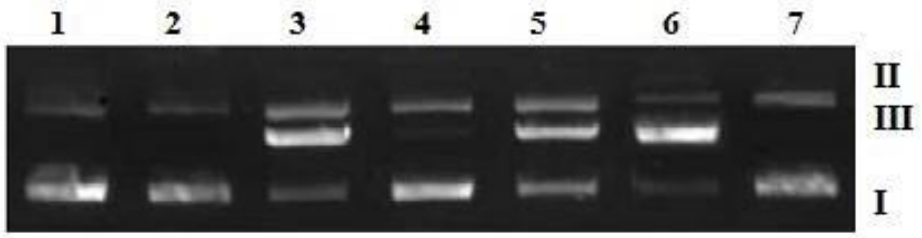

Figure 10. Gel electrophoresis diagrams showing the cleavage of supercoiled pBR322 DNA (150µg/ml) by copper (II) complex 4 (0.06 mM) in the presence of various agents in a 50 mM Tris–HCl buffer at pH 7.2 and 37 °C. Lane 1, DNA control; Lane 2, DNA + H_2O_2; Lane 3, DNA + H_2O_2+ complex 5; Lane 4,DNA + H_2O_2+ complex 5 + DMSO (1 mM); Lane 5, DNA+ H_2O_2+ complex 5+ NaN_3 ; Lane 6, DNA + H_2O_2+ complex 5+ SOD; Lane 7, DNA + H_2O_2 + complex 5+ KI.

3.6. Study of cytotoxicity by the MTT assay.

The MTT Cell Proliferation and Viability Assay is a reliable and sensitive in vitro method used to assess cell proliferation or a reduction in cell viability, which may occur due to apoptosis or necrosis. In this study, the MTT assay was used to evaluate the antineoplastic effects of the Cu(II) complexes 1, 3, and 5 on MCF-7 human breast cancer cells. The cytotoxic activity of these complexes was determined by treating the cells with various concentrations of the compounds, followed by thiazolyl blue tetrazolium bromide (MTT) colorimetric analysis (Figure 11).

The results demonstrated that complexes 1, 3, and 5 exhibited significant antineoplastic activity, with a marked decrease in cellular viability (Figure 12). Notably, the dicopper(II) complexes showed potent cytotoxic effects against MCF-7 cells, with IC_{50} values of 10.7 µM, 6.35 μM, and 4.08 μM for complexes 1, 3, and 5, respectively. These findings suggest that the cytotoxicity of the complexes increases with structural variation, particularly in complex 5, which showed the highest antiproliferative activity.

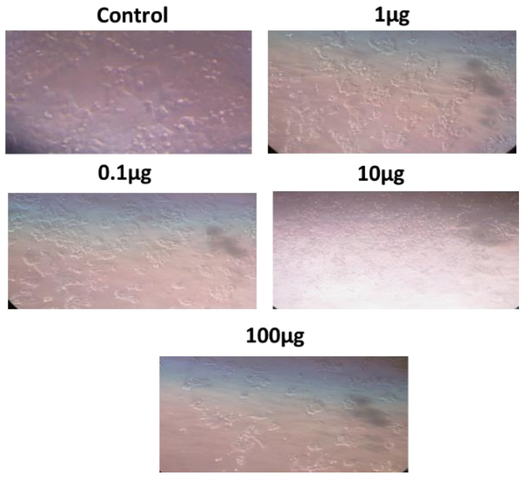

Figure 11. Morphology of Annexin V-FITC-stained MCF-7 breast cancer cells. Untreated cells(control) and treated cells with complex 5 at various concentrations.

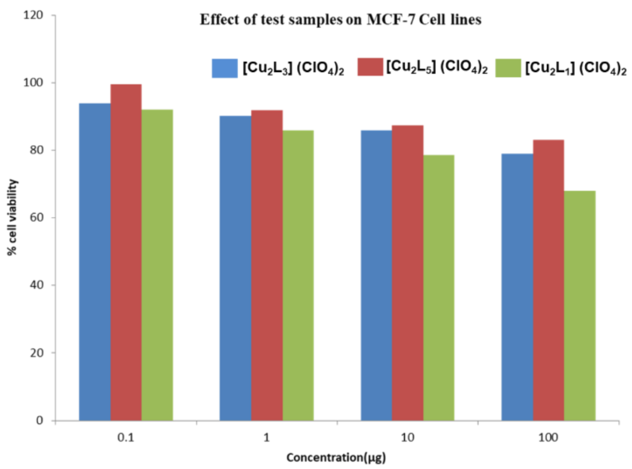

Figure 12. *In vitro* cytotoxicity of Cu(II) complexes at various concentrations in human breast (MCF-7)cancer cell lines – percentage of cell inhibition.

4. Conclusions

A novel series of binuclear Cu(II) complexes with unsymmetrical macrocyclic ligands was successfully synthesized and thoroughly characterized using various physicochemical and spectroscopic techniques, along with elemental analysis. Spectral studies confirmed that all complexes exhibit intercalative DNA binding and strong protein interactions, as evidenced by BSA fluorescence quenching via a static mechanism. Among them, complex 5 demonstrated markedly enhanced DNA-binding affinity and cleavage efficiency, attributed to π–π stacking interactions facilitated by the naphthalene-diamine-based macrocyclic ligand (L5), thereby enabling stronger intercalation into DNA.

DNA cleavage studies revealed that the complexes predominantly cleave DNA via an oxidative pathway. Notably, cleavage activity remained largely unaffected by reactive oxygen species (ROS) scavengers, including DMSO, KI, L-histidine, NaN_3, and SOD, suggesting a non-ROS-dependent mechanism. However, in some assays, especially in the presence of H_2O_2, oxidative cleavage involving hydroxyl radicals may contribute to the observed activity, although a hydrolytic component remains evident in the absence of oxidants.

Electrochemical analysis indicated quasi-reversible redox behavior across the series. Furthermore, MTT-based cytotoxicity assays revealed significant antiproliferative effects, particularly for complexes 1–3 and 5, against MCF-7 breast cancer cells, underscoring their potential as metal-based anticancer agents. Future research will focus on detailed mechanistic elucidation, in vivo validation, and structure–activity relationship studies to optimize therapeutic efficacy.

Author Contributions

Conceptualization, R. A. H.; Methodology, S. A. R., I. P., A. A., and H. T.; Software, S. A. R.; Investigation, S. A. R., I. P., A. A., and H. T.; Resources, V. S.; Data curation, R. A. H.; Writing – original draft, V. S.; Writing – review & editing, V. S., S. A. R., I. P., A. A., and H. T.; Supervision, V. S. All authors have read and agreed to the published version of the manuscript.

Institutional Review Board Statement

Not applicable. The study utilized publicly available data and did not involve direct human or animal participation.

Informed Consent Statement

Not applicable. This study did not involve human participants.

Data Availability Statement

The data supporting the findings of this study are available from the corresponding author upon reasonable request.

Funding

This research received no external funding.

Acknowledgments

The authors would like to acknowledge the support provided by their institution.

Conflicts of Interest

The authors declare no conflict of interest.

References

1. Ji, L.-N.; Zou, X.-H.; Liu, J.-G. Shape- and enantioselective interaction of Ru(II)/Co(III) polypyridyl complexes with DNA. *Coord. Chem. Rev.* **2001**, *216-217*, 513-536, https://doi.org/10.1016/S0010-8545(01)00338-1.
2. Vaidyanathan, V.G.; Nair, B.U. Synthesis, characterization and electrochemical studies of mixed ligand complexes of ruthenium(ii) with DNA. *Dalton Trans.* **2005**, 2842-2848, https://doi.org/10.1039/B502917A.
3. Pellegrini, P.P.; Aldrich-Wright, J.R. Evidence for chiral discrimination of ruthenium(ii) polypyridyl complexes by DNA. *Dalton Trans.* **2003**, 176-183, https://doi.org/10.1039/B208147D.
4. Maheswari, P.U.; Palaniandavar, M. DNA binding and cleavage activity of $[Ru(NH_3)_4(diimine)]Cl_2$ complexes. *norg. Chim. Acta* **2004**, *357*, 901-912, https://doi.org/10.1016/j.ica.2003.07.010.

5. Yang, X.-J.; Drepper, F.; Wu, B.; Sun, W.-H.; Haehnel, W.; Janiak, C. From model compounds to protein binding: syntheses, characterizations and fluorescence studies of $[Ru^{II}(bipy)(terpy)L]^{2+}$ complexes (bipy = 2,2′-bipyridine; terpy = 2,2′:6′,2″-terpyridine; L = imidazole, pyrazole and derivatives, cytochrome *c*). *Dalton Trans.* **2005**, 256-267, https://doi.org/10.1039/B414999H.
6. Tan, L.-F.; Wang, F.; Chao, H.; Zhou, Y.-F.; Weng, C. Ruthenium(II) mixed-ligand complex containing 2-(4′-benzyloxy-phenyl)imidazo[4,5-*f*][1,10]phenanthroline: Synthesis, DNA-binding and photocleavage studies. *J. Inorg. Biochem.* **2007**, *101*, 700-708, https://doi.org/10.1016/j.jinorgbio.2006.12.016.
7. Hambley, T.W. Developing new metal-based therapeutics: challenges and opportunities. *Dalton Trans.* **2007**, 4929-4937, https://doi.org/10.1039/B706075K.
8. Arnesano, F.; Natile, G. Mechanistic insight into the cellular uptake and processing of cisplatin 30 years after its approval by FDA. *Coord. Chem. Rev.* **2009**, *253*, 2070-2081, https://doi.org/10.1016/j.ccr.2009.01.028.
9. Jung, Y.; Lippard, S.J. Direct Cellular Responses to Platinum-Induced DNA Damage. *Chem. Rev.* **2007**, *107*, 1387-1407, https://doi.org/10.1021/cr068207j.
10. Zutphen, S.v.; Reedijk, J. Targeting platinum anti-tumour drugs: Overview of strategies employed to reduce systemic toxicity. *Coord. Chem. Rev.* **2005**, *249*, 2845-2853, https://doi.org/10.1016/j.ccr.2005.03.005.
11. Gust, R.; Beck, W.; Jaouen, G.; Schönenberger, H. Optimization of cisplatin for the treatment of hormone dependent tumoral diseases: Part 1: Use of steroidal ligands. *Coordination Chemistry Reviews* **2009**, *253*, 2742-2759, https://doi.org/10.1016/j.ccr.2009.02.025.
12. Gust, R.; Beck, W.; Jaouen, G.; Schönenberger, H. Optimization of cisplatin for the treatment of hormone-dependent tumoral diseases: Part 2: Use of non-steroidal ligands. *Coordination Chemistry Reviews* **2009**, *253*, 2760-2779, https://doi.org/10.1016/j.ccr.2009.02.029.
13. Bruijnincx, P.C.A.; Sadler, P.J. New trends for metal complexes with anticancer activity. *Curr. Opin. Chem. Biol.* **2008**, *12*, 197-206, https://doi.org/10.1016/j.cbpa.2007.11.013.
14. Sumi, M.; Nevaditha, N.T.; Sindhu Kumari, B. Synthesis, structural evaluation, antioxidant, DNA cleavage, anticancer activities and molecular docking study of metal complexes of 2-amino thiophene derivative. *J. Mol. Struct.* **2023**, *1272*, 134091, https://doi.org/10.1016/j.molstruc.2022.134091.
15. Ragheb, M.A.; Abdelrashid, H.E.; Elzayat, E.M.; Abdelhamid, I.A.; Soliman, M.H. Novel cyanochalcones as potential anticancer agents: apoptosis, cell cycle arrest, DNA binding, and molecular docking studies. *J. Biomol. Struct. Dyn.* **2025**, *43*, 9139-9157, https://doi.org/10.1080/07391102.2024.2316764.
16. Alniss, H.Y.; Al-Jubeh, H.M.; Msallam, Y.A.; Siddiqui, R.; Makhlouf, Z.; Ravi, A.; Hamdy, R.; Soliman, S.S.M.; Khan, N.A. Structure-based drug design of DNA minor groove binders and evaluation of their antibacterial and anticancer properties. *Eur. J. Med. Chem.* **2024**, *271*, 116440, https://doi.org/10.1016/j.ejmech.2024.116440.
17. Štarha, P.; Trávníček, Z.; Herchel, R.; Popa, I.; Suchý, P.; Vančo, J. Dinuclear copper(II) complexes containing 6-(benzylamino)purines as bridging ligands: Synthesis, characterization, and *in vitro* and *in vivo* antioxidant activities. *Inorg. Biochem.* **2009**, *103*, 432-440, https://doi.org/10.1016/j.jinorgbio.2008.12.009.
18. Oliveira, M.C.B.; Couto, M.S.R.; Severino, P.C.; Foppa, T.; Martins, G.T.S.; Szpoganicz, B.; Peralta, R.A.; Neves, A.; Terenzi, H. Nucleic acid cleavage by a Cu(II) polyaza macrocyclic complex. *Polyhedron* **2005**, *24*, 495-499, https://doi.org/10.1016/j.poly.2004.12.016.
19. Rupesh, K.R.; Deepalatha, S.; Krishnaveni, M.; Venkatesan, R.; Jayachandran, S. Synthesis, characterization and in vitro biological activity studies of Cu–M ($M=Cu^{2+}$, Co^{2+}, Ni^{2+}, Mn^{2+}, Zn^{2+}) bimetallic complexes. *Eur. J. Med. Chem.* **2006**, *41*, 1494-1503, https://doi.org/10.1016/j.ejmech.2005.11.016.
20. Lim, M.H.; Lau, I.H.; Barton, J.K. DNA Strand Cleavage near a CC Mismatch Directed by a Metalloinsertor. *Inorg. Chem.* **2007**, *46*, 9528-9530, https://doi.org/10.1021/ic701598k.
21. Pan, Z.-Q.; Ding, K.; Zhou, H.; Cheng, Q.-R.; Chen, Y.-F.; Huang, Q.-M. Syntheses, structures and properties of dinickel(II) macrocyclic complexes with two 2-thiophenoethyl pendant arms. *Polyhedron* **2011**, *30*, 2268-2274, https://doi.org/10.1016/j.poly.2011.06.004.
22. Saglam, N.; Colak, A.; Serbest, K.; Karaböcek, S.; Güner, S. DNA Hydrolysis by Homo- and Heteronuclear Cu(II)–Ni(II) Complexes of Two Diester-type Ligands. *Monatsh. Chem.* **2004**, *135*, 1023-1031, https://doi.org/10.1007/s00706-004-0178-6.
23. Kantacha, A.; Buchholz, R.; Smith, S.J.; Schenk, G.; Gahan, L.R. Phosphate ester cleavage promoted by a tetrameric iron(III) complex. *J. Biol. Inorg. Chem.* **2011**, *16*, 25-32, https://doi.org/10.1007/s00775-010-0696-0.

24. Vichard, C.; Kaden, T.A. Phosphate and phosphonate ester hydrolysis promoted by dinuclear metal complexes. *Inorg. Chim. Acta* **2002**, *337*, 173-180, https://doi.org/10.1016/S0020-1693(02)00997-0.
25. Kumar, A.; Ahmed, S.; Bhardwaj, M.; Imtiaz, S.; Kumar, D.; Bhat, A.R.; Sood, B.; Maji, S. *In vitro* anti-microbial, DNA-binding, *In silico* pharmacokinetics and molecular docking studies of Schiff-based Cu(II), Zn(II) and Pd(II) complexes. *J. Mol. Struct.* **2024**, *1315*, 138695, https://doi.org/10.1016/j.molstruc.2024.138695.
26. Guo, G.; Cui, C.; Hartanto, H.; Li, J.; Chen, T.-H. DNA polymerase mediated CRISPR/Cas12a trans-cleavage for dual-mode quantification of uracil DNA glycosylase activity. *Talanta* **2025**, *283*, 127089, https://doi.org/10.1016/j.talanta.2024.127089.
27. Rahaman, S.K.; Chatterjee, T.; Shaikh, K.; Khan, S.; Siddiqui, M.R.; Wabaidur, S.M.; Islam, M.M.; Alam, S.M.; Mir, M.H. Synthesis, structural elucidation, and DNA binding behavior of a ternary copper(II) complex featuring substituted bipyridyl and dicarboxylate ligands. *Polyhedron* **2025**, *266*, 117318, https://doi.org/10.1016/j.poly.2024.117318.
28. Fei, B.-L.; Tu, S.; Wei, Z.; Wang, P.; Long, J.-Y.; Qiao, C.; Chen, Z.-F. Biological evaluation of optically pure chiral binuclear copper(ii) complexes based on a rosin derivative as highly potential anticancer agents. *Dalton Trans.* **2019**, *48*, 15646-15656, https://doi.org/10.1039/C9DT01942A.
29. Sankar, N.; Devarajan, B.; Manimuthu, A.; Nattamai S.P, B.; Nallasamy, D.; Velusamy, K.M. Investigation on chloro-bridged binuclear copper(ii) complexes as potent metallodrug candidates against colon cancer *via* chemical and biological assessments. *New J. Chem.* **2024**, *48*, 3741-3757, https://doi.org/10.1039/D3NJ05335K.
30. Roy, A.; Khatun, S.; Dewale, P.D.; Rengan, A.K.; Chinta, J.P. Copper-assisted anticancer activity of hydroxycinnamic acid terpyridine conjugates on triple-negative breast cancer. *Dalton Trans.* **2024**, *53*, 18640-18652, https://doi.org/10.1039/D4DT02516D.
31. Panda, S.S.; Kumari, S.; Dixit, M.; Sharma, N.K. Synthesis and DNA cleavage studies of rationally designed metallopeptides from *N*-salicyl-AA-picolamide (SAP) and Cu(ii) ions. *New J. Chem.* **2024**, *48*, 19188-19194, https://doi.org/10.1039/D4NJ03573A.
32. Ressler, A.J.; Brandt, O.N.; Weaver, A.; Poor, J.E.; Ream, A.; Summers, N.A.; McMillen, C.D.; Seeram, N.P.; Dougherty, W.G.; Henry, G.E. Chromene-based Schiff base ligand: DNA interaction studies and characterization of tetranuclear zinc, nickel and iron complexes. *Inorg. Chim. Acta* **2023**, *547*, 121363, https://doi.org/10.1016/j.ica.2022.121363.
33. Aljohani, F.S.; El-Dabea, T.; El-Khatib, R.M.; Abdou, A.; Alzahrani, S.; Omar Barnawi, I.; El-Remaily, M.A.E.A.A.A.; Abu-Dief, A.M. Innovation, structural inspection for new mixed complexes: DNA binding, biomedical applications and molecular docking approaches. *J. Taibah Univ. Sci.* **2024**, *18*, 2350087, https://doi.org/10.1080/16583655.2024.2350087.
34. Sunitha, N.; Raj, C.I.S.; Kumari, B.S. Synthesis, spectral studies, biological evaluation and molecular docking studies of metal complexes from coumarin derivative. *J. Mol. Struct.* **2023**, *1285*, 135443, https://doi.org/10.1016/j.molstruc.2023.135443.
35. Retnam, C.T.G.; Rose, S.V.; Kumari, B.S. Synthesis, characterization, biological activity and molecular docking study of transition metal complexes from heterocyclic ligand system. *J. Mol. Struct.* **2023**, *1282*, 135162, https://doi.org/10.1016/j.molstruc.2023.135162.
36. Mahadevi, P.; Sumathi, S.; Dasgupta, S.; Noor, A. Bioactive benzhydrazone derived Schiff base and its metal(II) complexes: Synthesis, characterisation, cytotoxicity, DNA binding/cleavage, antimicrobial and antioxidant activity. *Inorg. Chem. Commun.* **2024**, *167*, 112800, https://doi.org/10.1016/j.inoche.2024.112800.
37. Mahadevi, P.; Sumathi, S.; Mehta, A. Ternary Schiff base metal (II) complexes with N,N,N′,N′-Tetramethylethylenediamine: Influence of secondary chelates on antimicrobial, scavenging activity, DNA interaction and cytotoxicity. *Polyhedron* **2024**, *255*, 116951, https://doi.org/10.1016/j.poly.2024.116951.
38. Gracelin Retnam, C.T.; Viola Rose, S.; Sindhu Kumari, B. Development of cancer-targeted nano gold functionalized ruthenium(III)-doxorubicin complex: Synthesis, characterization and evaluation of DNA cleavage, anticancer and bioimaging activity. *J. Mol. Liq.* **2024**, *401*, 124684, https://doi.org/10.1016/j.molliq.2024.124684.
39. Armarego, W.L.F.; Chai, C.L.L. Chapter 4 - Purification of Organic Chemicals. In Purification of Laboratory Chemicals (Sixth Edition), Armarego, W.L.F., Chai, C.L.L., Eds.; Butterworth-Heinemann: Oxford, **2009**; pp. 88-444, https://doi.org/10.1016/B978-1-85617-567-8.50012-3.

40. Gagne, R.R.; Spiro, C.L.; Smith, T.J.; Hamann, C.A.; Thies, W.R.; Shiemke, A.D. The synthesis, redox properties, and ligand binding of heterobinuclear transition-metal macrocyclic ligand complexes. Measurement of an apparent delocalization energy in a mixed-valent copper(I)copper(II) complex. *J. Am. Chem. Soc.* **1981**, *103*, 4073-4081, https://doi.org/10.1021/ja00404a017.
41. Al-Jeboori, M.J.; Hasan, H.A.; Jaafer Al-Sa'idy, W.A. Formation of polymeric chain assemblies of transition metal complexes with a multidentate Schiff-base. *Transit. Met. Chem.* **2009**, *34*, 593-598, https://doi.org/10.1007/s11243-009-9235-7.
42. Chen, J.; Wang, X.; Shao, Y.; Zhu, J.; Zhu, Y.; Li, Y.; Xu, Q.; Guo, Z. A Trinuclear Copper(II) Complex of 2,4,6-Tris(di-2-pyridylamine)-1,3,5-triazine Shows Prominent DNA Cleavage Activity. *Inorg. Chem.* **2007**, *46*, 3306-3312, https://doi.org/10.1021/ic0614162.
43. Wolfe, A.; Shimer, G.H., Jr.; Meehan, T. Polycyclic aromatic hydrocarbons physically intercalate into duplex regions of denatured DNA. *Biochemistry* **1987**, *26*, 6392-6396, https://doi.org/10.1021/bi00394a013.
44. Lee, M.; Rhodes, A.L.; Wyatt, M.D.; Forrow, S.; Hartley, J.A. GC base sequence recognition by oligoimidazolecarboxamide and C-terminus-modified analogs of distamycin deduced from circular dichroism, proton nuclear magnetic resonance, and methidiumpropylethylenediaminetetraacetate-iron(II) footprinting studies. *Biochemistry* **1993**, *32*, 4237-4245, https://doi.org/10.1021/bi00067a011.
45. Cohen, G.; Eisenberg, H. Viscosity and sedimentation study of sonicated DNA–proflavine complexes. *Biopolymers* **1969**, *8*, 45-55, https://doi.org/10.1002/bip.1969.360080105.
46. Ivanov, V.I.; Minchenkova, L.E.; Schyolkina, A.K.; Poletayev, A.I. Different conformations of double-stranded nucleic acid in solution as revealed by circular dichroism. *Biopolymers* **1973**, *12*, 89-110, https://doi.org/10.1002/bip.1973.360120109.
47. Mosmann, T. Rapid colorimetric assay for cellular growth and survival: Application to proliferation and cytotoxicity assays. *J. Immunol. Methods* **1983**, *65*, 55-63, https://doi.org/10.1016/0022-1759(83)90303-4.
48. Karunakaran, S.; Kandaswamy, M. Synthesis, electrochemical and magnetic properties of a series of new unsymmetrical macrocyclic binuclear copper(II) complexes. *J. Chem. Soc., Dalton Trans.* **1994**, 1595-1598, https://doi.org/10.1039/DT9940001595.
49. Johnston, D.H.; Glasgow, K.C.; Thorp, H.H. Electrochemical Measurement of the Solvent Accessibility of Nucleobases Using Electron Transfer between DNA and Metal Complexes. *J. Am. Chem. Soc.* **1995**, *117*, 8933-8938, https://doi.org/10.1021/ja00140a006.
50. Carter, M.T.; Bard, A.J. Voltammetric studies of the interaction of tris(1,10-phenanthroline)cobalt(III) with DNA. *J. Am. Chem. Soc.* **1987**, *109*, 7528-7530, https://doi.org/10.1021/ja00258a046.
51. Tian, J.-L.; Feng, L.; Gu, W.; Xu, G.-J.; Yan, S.-P.; Liao, D.-Z.; Jiang, Z.-H.; Cheng, P. Synthesis, crystal structure, magnetic property and nuclease activity of a new binuclear cobat(II) complex. *J. Inorg. Biochem.* **2007**, *101*, 196-202, https://doi.org/10.1016/j.jinorgbio.2006.08.009.
52. Liu, Y.; Wenning, L.; Lynch, M.; Reineke, T.M. New Poly($_D$-glucaramidoamine)s Induce DNA Nanoparticle Formation and Efficient Gene Delivery into Mammalian Cells. *J. Am. Chem. Soc.* **2004**, *126*, 7422-7423, https://doi.org/10.1021/ja049831l.
53. Uma Maheswari, P.; Palaniandavar, M. DNA binding and cleavage properties of certain tetrammine ruthenium(II) complexes of modified 1,10-phenanthrolines – effect of hydrogen-bonding on DNA-binding affinity. *J. Inorg. Biochem.* **2004**, *98*, 219-230, https://doi.org/10.1016/j.jinorgbio.2003.09.003.
54. Shao, Y.; Sheng, X.; Li, Y.; Jia, Z.-L.; Zhang, J.-J.; Liu, F.; Lu, G.-Y. DNA Binding and Cleaving Activity of the New Cleft Molecule *N,N'*-Bis(guanidinoethyl)-2,6-pyridinedicarboxamide in the Absence or in the Presence of Copper(II). *Bioconjugate Chem.* **2008**, *19*, 1840-1848, https://doi.org/10.1021/bc800062g.
55. Baguley, B.C.; Le Bret, M. Quenching of DNA-ethidium fluorescence by amsacrine and other antitumor agents: a possible electron-transfer effect. *Biochemistry* **1984**, *23*, 937-943, https://doi.org/10.1021/bi00300a022.
56. Li, F.-H.; Zhao, G.-H.; Wu, H.-X.; Lin, H.; Wu, X.-X.; Zhu, S.-R.; Lin, H.-K. Synthesis, characterization and biological activity of lanthanum(III) complexes containing 2-methylene–1,10-phenanthroline units bridged by aliphatic diamines. *J. Inorg. Biochem.* **2006**, *100*, 36-43, https://doi.org/10.1016/j.jinorgbio.2005.09.012.
57. Satyanarayana, S.; Dabrowiak, J.C.; Chaires, J.B. Tris(phenanthroline)ruthenium(II) enantiomer interactions with DNA: Mode and specificity of binding. *Biochemistry* **1993**, *32*, 2573-2584, https://doi.org/10.1021/bi00061a015.
58. Wittung, P.; Nielsen, P.; Nordén, B. Direct Observation of Strand Invasion by Peptide Nucleic Acid (PNA) into Double-Stranded DNA. *J. Am. Chem. Soc.* **1996**, *118*, 7049-7054, https://doi.org/10.1021/ja960521f.

59. Liu, J.; Zhang, T.; Lu, T.; Qu, L.; Zhou, H.; Zhang, Q.; Ji, L. DNA-binding and cleavage studies of macrocyclic copper(II) complexes. *J. Inorg. Biochem.* **2002**, *91*, 269-276, https://doi.org/10.1016/S0162-0134(02)00441-5.
60. Liu, J.-G.; Ye, B.-H.; Li, H.; Zhen, Q.-X.; Ji, L.-N.; Fu, Y.-H. Polypyridyl ruthenium(II) complexes containing intramolecular hydrogen-bond ligand: syntheses, characterization, and DNA-binding properties. *J. Inorg. Biochem.* **1999**, *76*, 265-271, https://doi.org/10.1016/S0162-0134(99)00154-3.
61. Shi, S.; Liu, J.; Li, J.; Zheng, K.-C.; Huang, X.-M.; Tan, C.-P.; Chen, L.-M.; Ji, L.-N. Synthesis, characterization and DNA-binding of novel chiral complexes Δ- and Λ-$[Ru(bpy)_2L]^{2+}$ (L=*o*-mopip and *p*-mopip). *J. Inorg. Biochem.* **2006**, *100*, 385-395, https://doi.org/10.1016/j.jinorgbio.2005.12.005.
62. Ghosh, K.S.; Sen, S.; Sahoo, B.K.; Dasgupta, S. A spectroscopic investigation into the interactions of 3′-*O*-carboxy esters of thymidine with bovine serum albumin. *Biopolymers* **2009**, *91*, 737-744, https://doi.org/10.1002/bip.21220.
63. Sathyadevi, P.; Krishnamoorthy, P.; Jayanthi, E.; Butorac, R.R.; Cowley, A.H.; Dharmaraj, N. Studies on the effect of metal ions of hydrazone complexes on interaction with nucleic acids, bovine serum albumin and antioxidant properties. *Inorg. Chim. Acta* **2012**, *384*, 83-96, https://doi.org/10.1016/j.ica.2011.11.033.
64. Ferrer, E.G.; Bosch, A.; Yantorno, O.; Baran, E.J. A spectroscopy approach for the study of the interactions of bioactive vanadium species with bovine serum albumin. *Bioorg. Med. Chem.* **2008**, *16*, 3878-3886, https://doi.org/10.1016/j.bmc.2008.01.060.
65. Urquiza, N.M.; Naso, L.G.; Manca, S.G.; Lezama, L.; Rojo, T.; Williams, P.A.M.; Ferrer, E.G. Antioxidant activity of methimazole–copper(II) bioactive species and spectroscopic investigations on the mechanism of its interaction with Bovine Serum Albumin. *Polyhedron* **2012**, *31*, 530-538, https://doi.org/10.1016/j.poly.2011.10.008.
66. Parsekar, S.U.; Paliwal, K.; Haldar, P.; Antharjanam, P.K.S.; Kumar, M. Synthesis, Characterization, Crystal Structure, DNA and HSA Interactions, and Anticancer Activity of a Mononuclear Cu(II) Complex with a Schiff Base Ligand Containing a Thiadiazoline Moiety. *ACS Omega* **2022**, *7*, 2881-2896, https://doi.org/10.1021/acsomega.1c05750.
67. Paliwal, K.; Haldar, P.; Antharjanam, P.K.S.; Kumar, M. Synthesis, Characterization, DNA/HSA Interaction, and Cytotoxic Activity of a Copper(II) Thiolate Schiff Base Complex and Its Corresponding Water-Soluble Stable Sulfinato–O Complex Containing Imidazole as a Co-ligand. *ACS Omega* **2023**, *8*, 21948-21968, https://doi.org/10.1021/acsomega.3c01853.

Publisher's Note & Disclaimer